Applicability of the sine-Gordon model to the magnetic heat capacity of $(C_6H_{11}NH_3)CuBr_3$

A. M. C. Tinus, W. J. M. de Jonge, and K. Kopinga
Department of Physics, Eindhoven University of Technology, P.O. Box 513, NL-5600 MB Eindhoven, The Netherlands
(Received 15 April 1985)

The field dependence of the magnetic heat capacity of $(C_6H_{11}NH_3)CuBr_3$ (CHAB), which is an ideal ferromagnetic $S=\frac{1}{2}$ chain system with XY anisotropy, is compared with predictions based on the sine-Gordon (sG) model and with transfer-matrix calculations on a chain of classical spins. A detailed analysis of the excess heat capacity in the region $1.5<T<7$ K and $B<7$ kG reveals systematic deviations from sG behavior. It is demonstrated that the spin components out of the XY plane have a rather pronounced effect. The importance of quantum effects in this $S=\frac{1}{2}$ system seems less than for $CsNiF_3$ and $(CH_3)_4NMnCl_3$ (TMMC), which is related to the relatively small (5%) XY anisotropy, together with the ferromagnetic intrachain interaction.

I. INTRODUCTION

Nonlinear effects have been shown[1] to play an important role in the static and dynamic properties of one-dimensional magnetic systems. Exact solutions, however, have only been obtained for a few special cases and, in general, yield hardly any information about the characteristics of the specific elementary excitations. An extensive theoretical and experimental effort was prompted by the observation[2] that, in the continuum limit, the equation of motion of both a ferromagnetic and an antiferromagnetic chain of classical spins with easy-plane anisotropy in a transverse field can—under certain approximations—be mapped to a sine-Gordon (sG) equation. Apart from linear excitations (magnons), this equation has solutions which are known as kink solitons.[3]

A variety of experiments on quasi-one-dimensional magnetic systems with easy-plane anisotropy have been interpreted in terms of the sG model. In particular, neutron scattering experiments, nuclear spin-lattice relaxation (NSLR), and heat capacity (C_p) measurements on both $CsNiF_3$ ($S=1$) (Refs. 4–6) and $(CH_3)_4NMnCl_3$ (TMMC, $S=\frac{5}{2}$) (Refs. 7–9) yielded indications of the existence of solitonlike excitations in these compounds in a certain field and temperature region. Recently, NSLR and C_p measurements on the $S=\frac{1}{2}$ system $(C_6H_{11}NH_3)CuBr_3$ (CHAB) (Ref. 10) were also interpreted in terms of solitons.

In general, the experimental results have been compared with predictions based upon an ideal-gas phenomenology, in which the solitons are assumed to behave as a dilute gas of noninteracting quasiparticles.[11] Although a satisfactory description of most of the data could be obtained, at least with a certain renormalization of the soliton rest energy, the validity of the sG approximation to real magnetic systems has been questioned by several authors.[12–14] In fact it is far from obvious whether the available data actually support evidence for the presence of solitons in the experimental systems, since in some cases the observed effects can also be explained in terms of other elementary excitations. On the other hand, it is not clear to which extent the various approximations involved with the mapping of the original magnetic system to a sG system affect a meaningful comparison of the latter model with the experimental data. In this paper we will analyze in detail the effects of these approximations on the interpretation of our heat capacity measurements on CHAB in terms of a sG model.

The organization of the paper is as follows. In Sec. II we discuss the implications of the ideal-gas phenomenology. The influence of out-of-plane spin components and the continuum limit will be considered in Sec. III by comparing the sG model with several appropriate classical model systems. In Sec. IV we estimate the influence of quantum effects, and compare some results from calculations on corresponding classical and $S=\frac{1}{2}$ systems. A comparison of various predictions for the field dependence of the magnitude and the location of the heat capacity maximum in CHAB with the data will be presented in Sec. V, together with a discussion, in which we briefly consider comparable data on $CsNiF_3$ and TMMC.

II. IDEAL-GAS PHENOMENOLOGY

We will start this section with a brief review of the most essential features of the magnetic properties of CHAB. Next, we will compare the available predictions for the heat capacity of the sG model and confront them with the experimental data on this compound.

Several investigations[15,16] revealed that CHAB is a system built up from very loosely coupled $S=\frac{1}{2}$ ferromagnetic chains, which to a very good approximation can be described by the Hamiltonian

$$H=-2J\sum_i[\mathbf{S}_i\cdot\mathbf{S}_{i+1}+(J_{zz}/J-1)S_i^zS_{i+1}^z]-g\mu_B\sum_i\mathbf{B}\cdot\mathbf{S}_i\ . \quad (1)$$

The intrachain interaction J/k amounts to 55 K; $J_{zz}/J=0.95$. In this Hamiltonian the small anisotropy within the XY plane $(J_{xx}-J_{yy})/J\simeq 10^{-3}$ (Ref. 16) is ignored. The y axis coincides with the crystallographic c axis of the orthorhombic system,[16] whereas the x axis is

located in the ab plane at an angle φ from the b axis. Two symmetry-related sets of chains are present with $\varphi=25°$ and $\varphi=-25°$, respectively. In this paper we confine ourselves to measurements with the external field **B** parallel to the c axis, which is located in the easy plane for both sets of chains. The interchain interactions, which are three orders of magnitude smaller than J/k, give rise to a three-dimensional long-range ordered state below $T_c=1.50$ K at $B=0$. In the paramagnetic region, the coupling between the chains can be neglected.[15]

The excess heat capacity ΔC for $1.5<T<7$ K, obtained by subtracting the zero-field data on CHAB from the data for $\mathbf{B}||c$, has recently been interpreted in terms of a sG model.[10] In close analogy to $CsNiF_3$ (Ref. 6) and TMMC (Ref. 9), this interpretation was based upon the ideal-gas phenomenology introduced by Krumhansl and Schrieffer,[11] in which the soliton contribution to the free energy per spin is proportional to the soliton density n_s:[3]

$$F=-kTn_s \quad \text{with } n_s=\left[\frac{8}{\pi}\right]^{1/2} mat^{-1/2}e^{-1/t} . \tag{2}$$

In this equation m denotes the soliton mass, a is the lattice spacing between adjacent spins, and $t=kT/E_s^0$, where E_s^0 is the soliton rest energy. For a system described by the Hamiltonian (1) with **B** in the XY plane, m and E_s^0 are given by:[17]

$$m=\frac{1}{a}(g\mu_B B/2JS)^{1/2}, \quad E_s^0=8S(2g\mu_B BJS)^{1/2} . \tag{3}$$

From Eq. (2) the soliton contribution ΔC_s to the excess heat capacity per spin can be obtained by straightforward differentiation as

$$\Delta C_s=\left[\frac{8}{\pi}\right]^{1/2} kmat^{-5/2}e^{-1/t}(1-t-\tfrac{1}{4}t^2) . \tag{4}$$

In comparing the sG model with experimental data on ΔC usually only the soliton contribution is considered. The magnon contribution to ΔC, which in this model is represented by a power series in t multiplied by kma, that should be added to Eq. (4), is neglected or replaced by its quantum-mechanical counterpart based on linear spin-wave theory.

At this point a comment on the ideal-gas phenomenology seems appropriate. In contrast to the evaluation of, e.g., the dynamic form factors $S(q,\omega)$ of the sG model, where explicit use is made of a formalism in which the solitons behave as an ideal gas of quasiparticles with density n_s, the calculation of the heat capacity only requires an expression for the total free energy F of the system. In this case the ideal-gas phenomenology may serve to identify the various contributions to the heat capacity, but, formally, has no effect on the calculations.

Some static properties of the sG model have been obtained more directly by Schneider and Stoll[18] from a numerical solution of the transfer integral equation of a discretized chain. The resulting prediction for ΔC is generally believed to be exact,[19,20] as was proved rigorously in the low- and high-temperature limits. In the so-called strong-coupling regime,[18] where the experiments on CHAB ($J/k=55$ K, $S=\frac{1}{2}$, $B<7$ kG) have been performed, these results show universal behavior, i.e., a plot of the *total* excess heat capacity $\Delta C/m$ against kT/E_s^0 yields a universal curve. In Fig. 1 this curve, labeled SS, is plotted, together with the total excess heat capacity based upon the ideal-gas phenomenology,[3,11] which is reflected by the dotted curve labeled KS,tot. The dashed curve labeled KS,sol represents the corresponding soliton contribution ΔC_s given in Eq. (4). From this figure one might conclude that the ideal-gas phenomenology leads to incorrect results for $t>0.15$, in which region the majority of the experimental data have been collected.

More recently, Sasaki and Tsuzuki[19] calculated the thermodynamic properties of the sG model within the ideal-gas phenomenology using a modified WKB method. The resulting expansion for the free energy can be associated with a magnon part, given by a power series in t, and a soliton part $-kTn_s$ with

$$n_s=\left[\frac{8}{\pi}\right]^{1/2} mat^{-1/2}e^{-1/t}(1-\tfrac{7}{8}t-\tfrac{59}{128}t^2+\ldots) . \tag{5}$$

Comparison of this equation with Eq. (2) reveals the presence of finite-temperature corrections to the density of kink solitons. The corresponding prediction for $\Delta C/m$, including the magnon part, is given by the dotted curve labeled ST1,tot in Fig. 1, and is in much better agreement with the numerical results than the original prediction.[3,11] Moreover, since the magnon contribution obtained by Sasaki and Tsuzuki is monotonically increasing for $t<0.3$, their results suggest that the maximum in ΔC calculated by Schneider and Stoll originates from the presence of kink solitons. The bare soliton contribution ob-

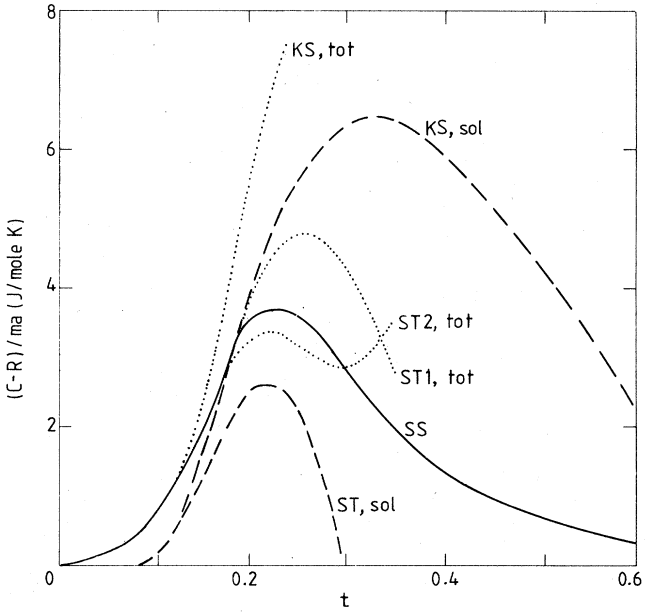

FIG. 1. Excess heat capacity of the sG model according to various theoretical approximations. The drawn curve reflects exact numerical results, whereas dotted curves denote estimates within the ideal-gas phenomenology. Dashed curves represent the bare soliton contribution. The first two letters of the labels of the various theoretical predictions refer to the corresponding authors, see the text.

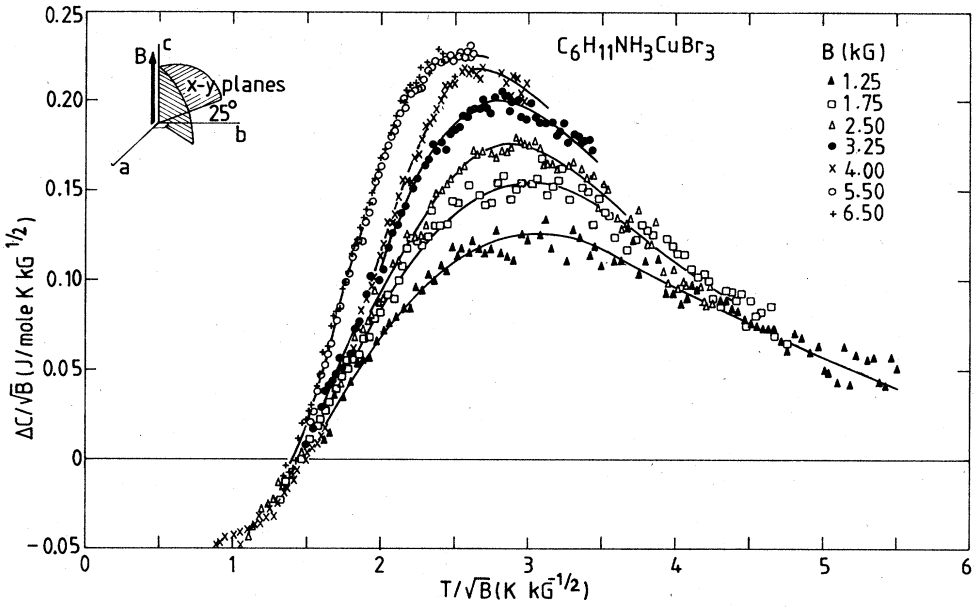

FIG. 2. Experimentally observed excess heat capacity of CHAB for $\mathbf{B}||c$ plotted in reduced form. Drawn curves are obtained by smooth interpolation of the data. The inset shows the orientation of the easy plane for the two symmetry-related sets of chains.

tained from Eq. (5) is represented by the dashed curve labeled ST,sol.

In a more detailed calculation, Sasaki and Tsuzuki included the effect of interactions between kink solitons.[21] The resulting total excess heat capacity is depicted in Fig. 1 by the dotted curve labeled ST2,tot. Although the inclusion of these interactions seems to yield a more accurate description of the heat capacity maximum itself, it is obvious that a somewhat irregular behavior occurs at $t\sim 0.3$.

We will now compare our experimental data on the excess heat capacity of CHAB with the predictions outlined above. For this purpose we plot the data which have already been reported before[10] in reduced form, i.e., $\Delta C/\sqrt{B}$ against $T/\sqrt{B}$. If the magnetic behavior of CHAB in the experimental field and temperature region can perfectly be represented by a sG model, this procedure should yield an universal curve, since for a ferromagnetic system both m and E_s^0 are proportional to $\sqrt{B}$ [cf. Eq. (3)]. Inspection of Fig. 2, where the experimental excess heat capacity is plotted in reduced form, clearly shows that the data collected at different fields do not collapse onto a single curve. For higher fields, the magnitude of $\Delta C/\sqrt{B}$ increases significantly, whereas the location of the maximum shifts to somewhat lower values of $T/\sqrt{B}$. Apart from this, the excess heat capacity becomes negative at low t, in contrast to the theoretical predictions outlined above. We will return to this point in Sec. IV.

The drawn curves in Fig. 2 are obtained by smooth interpolation of the various sets of data. For sake of clarity, only these curves are depicted in some of the following figures. In Fig. 3 the data are represented by dotted curves. In this figure we included several theoretical predictions, which will now successively be discussed. The dashed curve labeled 1 represents the soliton contribution to the excess heat capacity ΔC_s given by Eq. (4). In this equation we inserted the values of m and E_s^0 obtained from Eq. (3) with $J/k=55$ K, $g=2$, and $S=\frac{1}{2}$. The cor-

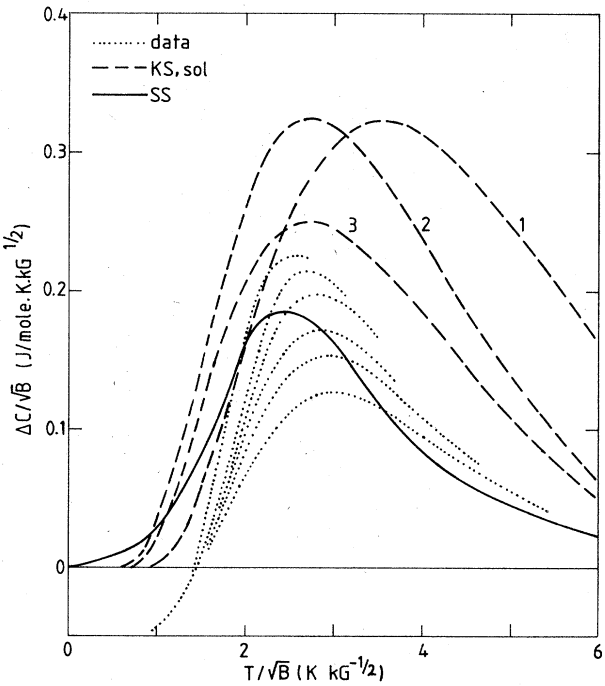

FIG. 3. The excess heat capacity of CHAB plotted in reduced form together with several theoretical predictions for a sG model. Dotted curves denote experimental data, whereas the drawn curve reflects exact numerical results. The dashed curves are explained in the text.

responding soliton rest energy E_s^0/k amounts to $10.85\sqrt{B}$ K (B in kG). The dashed curve labeled 3 denotes the prediction for ΔC which has been used in an earlier analysis[10] of the present data. Analogous to the original interpretation of the data on $CsNiF_3$ (Ref. 6) and TMMC (Ref. 9), that analysis was based on an expression for ΔC_s in which the properties of the system only enter through the parameter E_s^0. In fact, this expression is obtained directly from Eq. (4) by eliminating the soliton mass using the relation $m = E_s^0/(16aJS^2)$ [cf. Eq. (3)]. A fair overall description of the data was obtained with a renormalization of the parameter E_s^0/k by 20% to $8.4\sqrt{B}$. It is obvious that such a procedure implicitly yields also a reduction of the soliton mass by 20%. The effect of a renormalization of the soliton rest energy in Eq. (4) to $8.4\sqrt{B}$ *without* changing m is reflected in Fig. 3 by the dashed curve labeled 2. Although accurate quantitative predictions for the renormalization of E_s^0 and m are not available (cf. Sec. IV) the previously reported fair agreement of the theory with the data seems rather fortituous, since the corresponding expression for the excess heat capacity [cf. Eq. (4)] is not valid in the present temperature region, as was demonstrated above.

A much better quantitative description of the data is provided by the numerical results of Schneider and Stoll,[18] which are represented in Fig. 3 by the drawn curve labeled SS. As we already mentioned above, these results include *all* contributions to the excess heat capacity of the sG model, in contrast to the other theoretical predictions plotted in this figure, which only represent the contribution from kink solitons within the framework of the original ideal-gas phenomenology.[3] It is obvious that the (exact) numerical results, corresponding in Fig. 3 to $E_s^0/k = 10.85\sqrt{B}$ [cf. Eq. (3)], agree fairly well with the "average" data. Hence we conclude that a correct description of the excess heat capacity of CHAB in terms of a sG model does not require a significant renormalization of the soliton rest energy. Our data even suggest a small increase of E_s^0 with respect to the "classical" value rather than the decrease inferred above. We will return to this point in Sec. IV. On the other hand, inspection of Fig. 3 reveals that the sets of data collected at different fields show systematic deviations from the numerical results for the sG model. In the next section we will demonstrate that this nonuniversal behavior, which was already noted above, most likely originates from the effect of spin components out of the easy plane.

III. OUT-OF-PLANE SPIN COMPONENTS

In the foregoing section we have shown that the experimental data on CHAB exhibit systematic deviations from the exact numerical results for the excess heat capacity of the sG model. Since these results, in principle, are obtained without any additional assumptions, such as the ideal-gas phenomenology, it is evident that the observed deviations originate from the various approximations involved in the mapping of the original equation of motion of the spins to a sG equation. However, the effect of each individual approximation on the theoretical prediction for ΔC is far from obvious. These approximations can be summarized as follows: the spins are treated as classical vectors, the anisotropy is large enough to confine the motion of the spins to an easy plane, and the limit of zero lattice spacing is taken.

Recently, several corrections for the static and dynamic properties predicted by the sG model have been proposed[22–24] in order to account for the out-of-plane spin components. As the calculation of the heat capacity formally does not require a knowledge of the properties of the individual elementary excitations, we will confine ourselves here to a direct approach, in which the excess heat capacity is compared with exact numerical results for ΔC obtained from transfer-matrix calculations on a chain of classical spins in a transverse field.[25] In these calculations the known exchange and anisotropy parameters of CHAB are used. The results are represented by the drawn curves in Fig. 4, in which we also plotted the smoothed experimental data (dashed curves). Inspection of this figure shows that the magnitude of ΔC obtained from the transfer-matrix calculations is too high by about a factor 2. Nevertheless, the systematic deviations of the data from "universal" behavior, i.e., the increase of the magnitude of the maximum of $\Delta C/\sqrt{B}$ and the shift of the maximum towards lower values of $T/\sqrt{B}$ at higher fields, are predicted correctly. Hence we conclude that these features very likely originate from out-of-plane spin components.

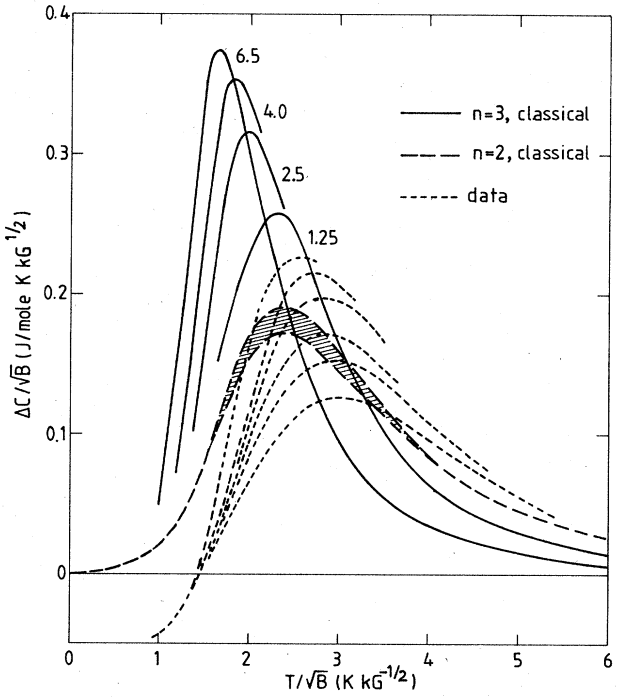

FIG. 4. The excess heat capacity of CHAB plotted in reduced form, together with numerical results of transfer-matrix calculations on a classical spin system. Drawn curves, characterized by the magnitude of the magnetic field, represent calculations on a system in which the spins have three components. The shaded area represents calculations for $1.25 < B < 6.5$ kG on a planar system, in which the spins have only two nonzero components.

The present approach, however, has the formal drawback that it may be somewhat obscured by the effects of the continuum limit, since the transfer-matrix calculations are performed for a discrete chain. To discriminate between the effects of out-of-plane spin components and the continuum limit, it would be useful to compare the exact numerical results for the excess heat capacity of the sG model with transfer-matrix calculations on a chain of classical spins in a transverse field, in which the importance of the out-of-plane spin components is varied by the value of J_{zz} ($0 \leq J_{zz} \leq J$), especially in the limit $J_{zz}=0$. Unfortunately, such calculations give rise to numerical problems at low values of kT/J if J_{zz} differs significantly from J.[25] Therefore, we have to resort to transfer-matrix calculations on a planar ($n=2$) system, i.e., a chain of classical spins which are fully confined to the XY plane. Note that this system is essentially different from the $n=3$ model in the limit $J_{zz}=0$ mentioned above, where the spins still can have an (energetically unfavorable) out-of-plane component. The results of these $n=2$ transfer-matrix calculations for $J_{xx}/k=J_{yy}/k=55$ K are reflected by the shaded area in Fig. 4, bounded by broken curves, the upper and lower curve corresponding to $B=6.5$ kG and $B=1.25$ kG, respectively. We like to note that inclusion of the small in-plane anisotropy $(J_{xx}-J_{yy})/J \simeq 10^{-3}$ has no significant effect on the results for ΔC, which conclusion also holds for the $n=3$ case.

The numerical results of Schneider and Stoll for the excess heat capacity of the sG model are located within the shaded area in Fig. 4, and coincide with the $n=2$ transfer-matrix results for $B=4$ kG within a few percent. The good agreement between the results for these two model systems indicates that the influence of the continuum limit on the excess heat capacity is rather small in the present field region. Of course, the small deviations of the $n=2$ results from universal behavior might be associated with lattice discreteness effects, but such a conclusion should be considered with some reservations, since the best agreement of the numerical results for the discrete $n=2$ system with those for the sG model does not occur at the lowest field, where the influence of the discrete lattice spacing should be minimal, because in this region the kink solitons have their maximum length. Nevertheless, the evidence presented in Fig. 4 strongly suggests that the influence of the continuum limit is rather unimportant compared with that of the out-of-plane spin components. The quantitative effect of these spin components on ΔC seems to increase dramatically at higher fields, as can be inferred from a comparison of the numerical results for the discrete $n=3$ and $n=2$ systems. In the next section we will consider the influence of quantum effects on the present analysis.

IV. QUANTUM EFFECTS

Especially at low temperatures, the heat capacity is very sensitive to quantum effects, since it directly probes the location of the energy levels of the system. A trivial demonstration of this fact is the heat capacity of the $1d$ classical spin model, which approaches the value Nk_B at $T=0$ instead of zero, thus violating the third law of thermodynamics.[26] On the other hand, the kink solitons occurring in a sG system behave as quasiparticles with a finite rest energy. Since these solitons are not present in zero field, it is not *a priori* impossible that the classical sG model—despite its inadequacy to describe the total heat capacity of a quantum system—may give a fair description of the excess heat capacity ΔC, at least in that field and temperature region where the solitons have sufficient statistical weight. This assumption is supported by the experimental evidence presented in the preceeding sections.

In the remaining part of this section we shall first consider the effect of several quantum corrections that have been proposed for the sG model, especially for the range of parameters appropriate to CHAB. Next, we will illustrate the potential influence of quantum effects by comparing the excess heat capacity of the classical and $S=\frac{1}{2}$ anisotropic XY systems.

The inclusion of quantum effects in the sG model has been considered by several authors.[27–29] Their calculations reveal that the importance of quantum effects is related to the magnitude of the coupling parameter $g^2=c_0/E_0$, where for the present system $E_0=2JS^2a$ and c_0 is the so-called magnon velocity. This parameter is often rewritten as $g^2=8m^*/E_s^0$, where m^* is the magnon gap and E_s^0 is given by Eq. (3). If g^2 is small compared to unity, the behavior of the system can be described by semiclassical statistics, and only a renormalization of the soliton energy and the mass parameter is required. For a ferromagnetic system described by the Hamiltonian (1), $g^2=\sqrt{2}/S(1-J_{zz}/J)^{1/2}$, yielding the value $g^2=0.62$ for CHAB.

If we use the expressions given by Maki,[27] we obtain a reduction of both E_s^0 and m by about 10% in the field region of interest. This renormalization shifts both the magnitude and the location of the predicted maximum excess heat capacity to lower values, thus increasing the deviations between the numerical results for the sG model and the experimental data presented in Fig. 3. One should note, however, that in the mapping of the spin system to a sG model (cf. Sec. II) the length of the classical spin vector is taken equal to the spin quantum number S. If, alternatively, one starts from the semiclassical value $\hat{S}=\sqrt{S(S+1)}$ the "initial" predictions for E_s^0 and m would be substantially higher, and hence the proposed quantum corrections would improve the description of the data.

Mikeska[28] has analyzed the quantum effects in a sG model allowing small deviations from idealized planar behavior. For anisotropies that are characteristic for the experimental systems investigated up till now, he obtains a reduction of the soliton rest energy which only depends on the value of S. In his analysis, the classical estimates for E_s^0 and m are given by expressions similar to Eq. (3), where S has been replaced by $\hat{S}$. The net result of the inclusion of quantum effects on the numerical results for the sG model plotted in Fig. 3 is a decrease of $\Delta C/\sqrt{B}$ and the value of $T/\sqrt{B}$ at which the maximum excess heat capacity occurs by about 30% and 5%, respectively. This renormalization does not result in a better description of the experimentally observed excess heat capacity,

except for the lowest fields. Probably, the better agreement at lower fields is related to the smaller influence of the out-of-plane spin components in this region (cf. Sec. III), which very likely improves the description of the experimental system in terms of the sG model, but, actually, the available evidence does not permit any quantitative conclusions about the validity of the suggested quantum corrections.

Riseborough[29] has shown that, in principle, the quantum effects in a discrete lattice may differ considerably from those calculated within a continuum approximation. However, his analysis reveals that the various corrections involved with lattice discreteness cancel in numerical estimates based on parameter values that have been extracted from the spin-wave dispersion relation. It is not clear, however, whether this conclusion also holds for the present system, where the estimates for the various parameters are partly based on heat-capacity measurements in the paramagnetic region.[15]

We wish to emphasize that the good description of the average excess heat capacity of CHAB by the exact numerical results for a classical sG model does not necessarily imply that the bare quantum effects in this experimental system are small. In fact, these effects significantly reduce the excess heat capacity, as can be inferred directly from Fig. 4 by comparing the experimental data with the $n=3$ transfer-matrix results, which are calculated for the same Hamiltonian and the same parameters[15,16] that describe the chains in CHAB, except for the fact that the spins are represented by classical vectors. The good description of the average data by a sG model most likely arises from a compensation of the influence of out-of-plane spin components, which tend to increase the excess heat capacity, by the influence of quantum effects, which result in a decrease of ΔC. Within the framework of the sG model, the predicted quantum corrections are rather small for the range of parameters corresponding to the experiments on CHAB, as was shown above. This suggests that also in these theoretical calculations the potential quantum nature of the present $S=\frac{1}{2}$ system is to a large extent "neutralized" by the relatively small XY anisotropy, which is reflected by the small value of the coupling parameter $g^2=0.62$. This view is supported by the results obtained by Wysin *et al.*[30] from a numerical simulation of the soliton dynamics. They conclude that the deviation of the behavior of CHAB from sG theory originates from finite excursions of spins away from the easy plane, whereas, because of the small XY anisotropy, the quantum effects are weaker than in the $S=1$ system $CsNiF_3$.

The rather crucial influence of the amount of XY anisotropy can be illustrated by a theoretical comparison of the classical and $S=\frac{1}{2}$ anisotropic XY systems. Both systems are described by the Hamiltonian

$$H=-2J\sum_i[(1+\gamma)S_i^xS_{i+1}^x+(1-\gamma)S_i^yS_{i+1}^y] \qquad (6)$$

and can be solved rigorously. The static properties of the classical system are calculated by a transfer-matrix method, whereas the $S=\frac{1}{2}$ system can be mapped on a system of noninteracting fermions by invoking the Wigner-Jordan transformation.[31] The symmetry within the easy plane is broken by an orthorhombic anisotropy characterized by γ, which actually replaces the action of the usual transverse magnetic field. In the classical case, the system described by Eq. (6) can be mapped on a sG system,[32] in which π solitons are allowed. The excess heat capacity $\Delta C=C(\gamma)-C(\gamma=0)$ is plotted in Fig. 5 for both the classical and the $S=\frac{1}{2}$ model. The dashed curve reflects the numerical calculations by Schneider and Stoll for a sG model. Their results agree very well with those for the classical system described by Eq. (6); the small deviations are most likely due to lattice discreteness effects. A comparison of the classical and $S=\frac{1}{2}$ systems presented in Fig. 5 reveals that, although the maximum excess heat capacity occurs at comparable temperatures for both systems, the magnitude of ΔC differs up to a factor of 40. This discrepancy must be related to the large XY anisotropy of the system described by the Hamiltonian (6).

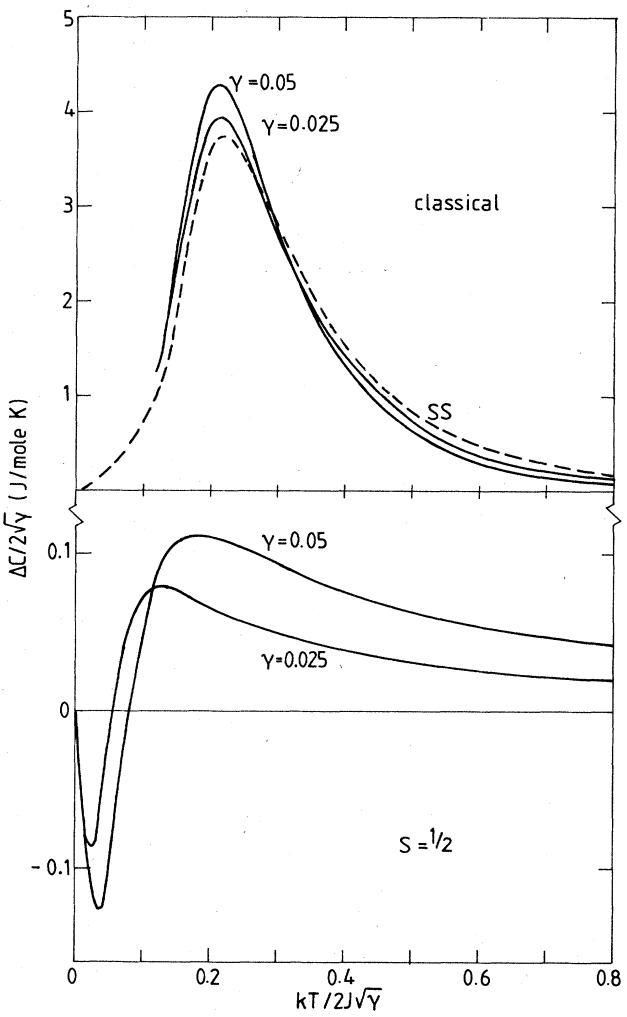

FIG. 5. Excess heat capacity of a classical and an $S=\frac{1}{2}$ XY linear chain system, plotted in reduced form. The curves are characterized by the relative anisotropy within the XY plane. The dashed curve represents exact numerical results for a sG model.

Within the framework of the theoretical calculations of the quantum corrections for a sG model discussed above, the value of the coupling parameter g^2 of these systems amounts to $8\sqrt{2}$, which indeed invalidates the use of (semi)classical statistics.

We conclude this section with the remark that the small magnitude of ΔC in the $S=\frac{1}{2}$ XY case might already have been anticipated from the magnetic entropy of the system. It is well-known that the presence of a field or anisotropy enhances the magnetic order, i.e., it gives rise to an increase of the correlations between some of the spin components and a shift of the entropy S towards higher temperatures. Since S is equal to the integral of C/T, a positive excess heat capacity in a certain temperature region in fact results from the fraction of entropy removed at lower temperatures. In the $S=\frac{1}{2}$ isotropic XY system the amount of entropy below the temperature region of interest ($kT/J<0.05$) is very small.[33] This limits ΔC to low values, in contrast to the classical system, where formally an infinite amount of entropy is present at $T=0$. The shift of entropy produced by a field or anisotropy also explains the fact that the experimental excess heat capacity plotted in Fig. 2 becomes negative at low temperatures, as was already noted in Sec. II. The same holds for the $S=\frac{1}{2}$ XY system presented above.

V. DISCUSSION

In the preceeding sections we have shown that the overall behavior of the excess heat capacity of CHAB in the region $1.5<T<7$ K and $1.25<B<7$ kG can be described fairly well by the exact numerical results for the sG model.[18] In the present section we will focus our attention to the location and the magnitude of the maximum of $\Delta C/\sqrt{B}$, and compare the experimental evidence with several theoretical predictions. Next, we will compare the results of our analysis of the data on CHAB with those for two other potentially soliton-bearing systems, $CsNiF_3$ and TMMC.

In Fig. 6 the reduced maximum excess heat capacity $\Delta C_m/\sqrt{B}$ and the temperature $T_m/\sqrt{B}$ at which this maximum occurs are plotted against the external field B. The experimental data are denoted by open circles; the dotted curves are guides to the eye. We first discuss the field dependence of $\Delta C_m/\sqrt{B}$.

The horizontal line labeled KS,sol1 reflects the soliton excess heat capacity of the sG model given by Eq. (4). This prediction is systematically higher than the data, as was noted already in Sec. II. The effect of the renormalization of the soliton rest energy as reported in our previous analysis[10] is indicated by the line labeled KS,sol3. A much better description is obtained by, alternatively, the exact numerical results for the sG model (SS) or the $n=2$ classical model. All these theoretical approaches, however, do not predict a significant increase of $\Delta C_m/\sqrt{B}$ with field, as displayed by the data. In Sec. III we pointed out that this increase originates from out-of-plane spin components. This is demonstrated very nicely by the curve labeled $n=3$ in Fig. 6. This prediction, which is obtained from transfer-matrix calculations on a classical spin model, actually gives an almost perfect qualitative description of the observed field dependence. Within the

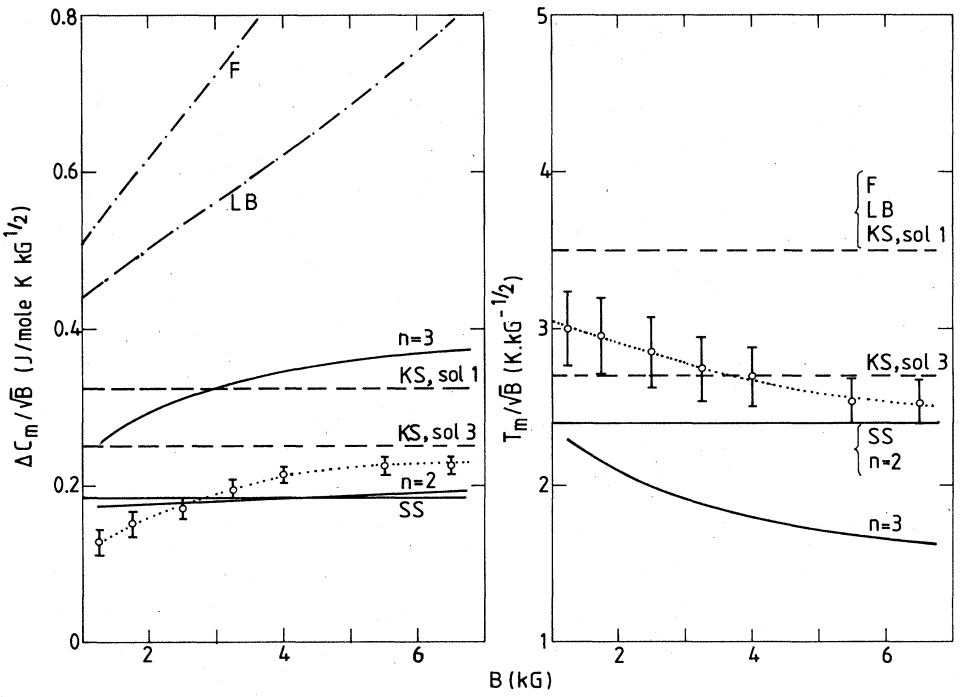

FIG. 6. Field dependence of the reduced maximum excess heat capacity $\Delta C_m/\sqrt{B}$ (left) and the reduced temperature $T_m/\sqrt{B}$ at which this maximum occurs (right). Open circles are the experimental data on CHAB; the dotted curves are guides to the eye. The various theoretical predictions are discussed in the text.

ideal-gas phenomenology, the out-of-plane spin components have been included in the theory by Fogedby[23] (F) and by Leung and Bishop[22] (LB), using a steepest descent method and a path-integral method, respectively. Although these approaches yield a correct field dependence of $\Delta C_m/\sqrt{B}$ at low fields, the resulting magnitude of the excess heat capacity is far too high.

A comparison of the field dependence of $T_m/\sqrt{B}$ with the available theoretical predictions leads to largely similar conclusions. Predictions based on the sG model all result in horizontal lines. We wish to note that the dashed line labeled KS,sol3 describes the data almost within experimental inaccuracy. In our original interpretation, where ΔC at a fixed temperature was plotted against B, the systematic deviations which seem evident now were not observed, due to the limited number of data in these plots. A correct qualitative description of the observed field dependence is again only given by the $n=3$ classical spin model, in which the out-of-plane spin components are fully taken into account. The difference between this prediction and the experimental data on CHAB actually reflects the bare influence of quantum effects on the excess heat capacity in this compound, as was already noted in Sec. IV.

In view of the results of the analysis of the excess heat capacity of CHAB, it seems interesting to analyse the behavior of ΔC of two other potentially soliton-bearing systems, $CsNiF_3$ and TMMC, in a similar way. In Fig. 7 we therefore present the reported[6] excess heat capacity of $CsNiF_3$ as a plot of $\Delta C/\sqrt{B}$ against $T/\sqrt{B}$. In this figure we also included the numerical results for the sG model, based on the reported value of the intrachain interaction $J/k=11.8$ K.[4] Although the scatter of the data is rather large, the sets of data collected at different fields seem to display only small deviations from universal behavior. In particular, the maximum value of $\Delta C/\sqrt{B}$ is almost independent of the applied field. As we demonstrated in Sec. III, this indicates that the influence of out-of-plane spin components is rather small, which is not inconsistent with the relatively large value of the easy-plane anisotropy in this compound [$A/J=0.2$; classical value of A (Ref. 4)]. As a result of this large anisotropy, the quantum effects in this system might be rather important. Within the framework of the sG model, the decrease of ΔC due to quantum effects (cf. Sec. IV) may be substantially larger than the increase resulting from out-of-plane spin components. This is corroborated by the evidence presented in Fig. 7, which shows that the magnitude of the experimentally observed excess heat capacity is lower than the numerical results for the sG model by about a factor 2. Such a reduction is considerably larger than the theoretical predictions,[27–29] which yield a renormalization of both E_s^0 and the mass parameter by 10—20% for this system. This discrepancy suggests that $CsNiF_3$ cannot properly be described by semiclassical statistics. A more or less similar conclusion has recently been drawn by Pini *et al.*[14] from a comparison of the excess heat capacity of this compound with the results of $n=3$ transfer-matrix calculations for a chain of classical spins.

Next, we will consider TMMC. For an antiferromagnetic system, both E_s^0 and m are proportional to B. Therefore we presented the data collected by Borsa[9] as a plot of $\Delta C/B$ against T/B in Fig. 8, where we also included the exact numerical results for a sG model,[18] based on an intrachain interaction $J/k=-6.7$ K. Inspection of this figure shows that the reduced temperature at

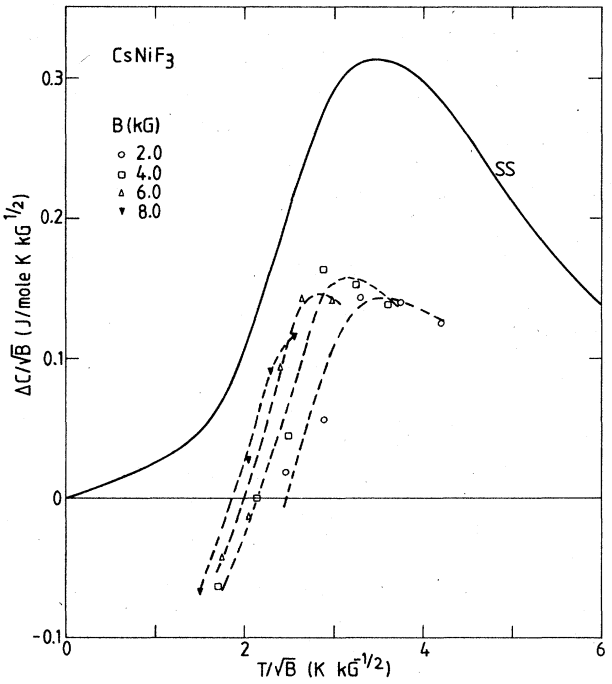

FIG. 7. Experimentally observed excess heat capacity of $CsNiF_3$ according to Ramirez and Wolf (Ref. 6) plotted in reduced form. The drawn curve represents the corresponding exact numerical results for a sG model.

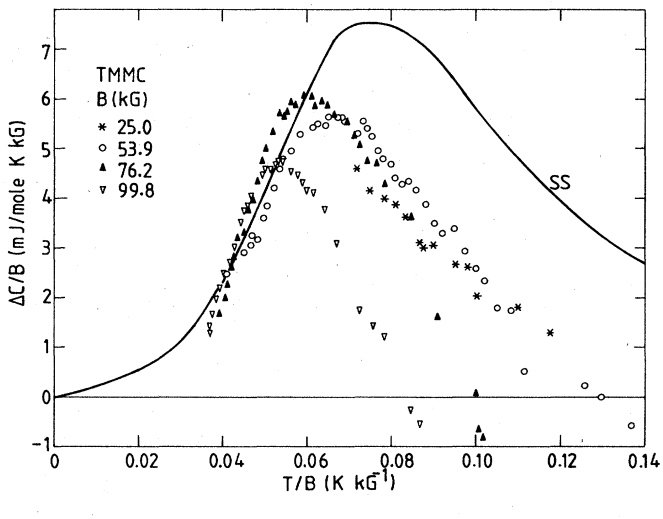

FIG. 8. Experimentally observed excess heat capacity of TMMC according to Borsa (Ref. 9) plotted in reduced form. The drawn curve represents the corresponding exact numerical results for a sG model.

which the maximum experimental excess heat capacity occurs decreases significantly at higher fields. As we pointed out in Sec. III, such a decrease may arise from the presence of out-of-plane spin components. For TMMC this is not unlikely, given the very small easy-plane anisotropy ($<2\%$) in this compound, compared to CHAB (5%) and $CsNiF_3$ (20%). However, the magnitude of $\Delta C/B$ does not increase with field, as expected (cf. Sec. III), but it decreases dramatically at the highest field. According to Borsa *et al.*,[20] this indicates the inadequacy of the sG model in this field region, although they obtain a better quantitative agreement with theory if the experimental excess heat capacity is corrected for the magnon contribution, which may be as large as $-0.2J$/mole K in TMMC. Nevertheless, the maximum excess heat capacity is systematically lower than the numerical results for the sG model, suggesting that the decrease of $\Delta C/B$ due to quantum effects is so large that it "overcompensates" the increase expected from out-of-plane spin components.

The importance of quantum effects in this system is also reflected by the temperature at which the maximum excess heat capacity occurs. For a correct description of this temperature within the framework of the sG model, the soliton rest energy has to be renormalized by about 20%. This value agrees very well with the renormalization of 21% inferred from neutron scattering experiments,[7] suggesting that the quantum effects are indeed rather pronounced. Given the spin quantum number $S=\frac{5}{2}$ for TMMC and the small value of the easy-plane anisotropy, this must be related to the fact that this compound is built up from *antiferromagnetic* chains. These chains have a large zero-point spin reduction,[34] which gives rise to a renormalization of the magnon gap and hence the parameters in the sG model with respect to their classical values. Within the framework of the sG model, a renormalization of the magnon gap by about 30% is predicted for TMMC.[27] This renormalization has about the same magnitude as that inferred from detailed antiferromagnetic resonance experiments[34] on this compound.

We conclude this discussion on TMMC by noting that the importance of out-of-plane spin components is also demonstrated by Fowler *et al.*,[35] who calculated the excess heat capacity of this system from quantum-sine-Gordon thermodynamics. Their prediction for ΔC is about a factor 2 lower than the experimental data, suggesting that the rest of the energy goes into out-of-plane modes. They also report that, in contrast to the sG prediction, no significant renormalization of the magnon gap occurs. Although this conclusion seemed justified by the neutron scattering results of Heilmann *et al.*[36] it disagrees with the antiferromagnetic resonance results mentioned above. The reason for this discrepancy is not clear.

Finally, we would like to comment on the implications of the present analysis for the interpretation of experiments on the dynamic properties within the framework of the sG model. In contrast to the theoretical evaluation of the dynamic form factors $S(q,\omega)$, the calculation of the heat capacity does, formally, not require a detailed knowledge of the individual elementary excitations, as we already noted in Sec. II. Nevertheless, a comparison of the predictions of Sasaki and Tsuzuki for the heat capacity of the sG model with the numerical results of Schneider and Stoll reveals that kink solitons have a statistical weight comparable to that of the other excitations in the field and temperature region where the majority of experimental data have been collected. This is corroborated by neutron scattering, nuclear spin-lattice relaxation, and Mössbauer experiments, which reveal contributions to $S(q,\omega)$ that can be attributed to solitons. All these experiments, however, have been interpreted in terms of an ideal-gas phenomenology using expressions for n_s [Eq. (4)] that are only valid at $kT/E_s^0<0.15$. Although our analysis indicates that the applicability of the sine-Gordon model to the actual experimental systems is limited by out-of-plane spin components and quantum effects, it may be worthwhile to reanalyze the data using expressions for n_s in which finite temperature corrections are included.

ACKNOWLEDGMENTS

We wish to thank F. Borsa for putting the original data on TMMC at our disposal and H. C. Fogedby for communication of his results and some stimulating discussions.

[1]See, for instance, J. D. Johnson and J. C. Bonner, Phys. Rev. B **22**, 251 (1980), and references therein.
[2]H. J. Mikeska, J. Phys. C **11**, L29 (1978); **13**, 2913 (1980).
[3]J. F. Currie, J. A. Krumhansl, A. R. Bishop, and S. E. Trullinger, Phys. Rev. B **22**, 477 (1980).
[4]For a detailed report, see M. Steiner, K. Kakurai, and J. K. Kjems, Z. Phys. B **53**, 117 (1983).
[5]T. Goto and Y. Yamaguchi, J. Phys. Soc. Jpn. **50**, 2133 (1981).
[6]A. P. Ramirez and W. P. Wolf, Phys. Rev. Lett. **49**, 227 (1982).
[7]L. P. Regnault, J. P. Boucher, J. Rossat-Mignod, J. P. Renard, J. Bouillot, and W. G. Stirling, J. Phys. C **15**, 1261 (1982).
[8]J. P. Boucher and J. P. Renard, Phys. Rev. Lett. **45**, 486 (1980).
[9]F. Borsa, Phys. Rev. B **25**, 3430 (1982).
[10]K. Kopinga, A. M. C. Tinus, and W. J. M. de Jonge, Phys. Rev. B **29**, 2868 (1984).
[11]J. A. Krumhansl and J. R. Schrieffer, Phys. Rev. B **11**, 3535 (1975).
[12]J. M. Loveluck, T. Schneider, E. Stoll, and J. Jauslin, Phys. Rev. Lett. **45**, 1505 (1981).
[13]G. Reiter, Phys. Rev. Lett. **46**, 202 (1981).
[14]M. G. Pini and A. Rettori, Phys. Rev. B **29**, 5246 (1984).
[15]K. Kopinga, A. M. C. Tinus, and W. J. M. de Jonge, Phys. Rev. B **25**, 4685 (1982).
[16]A. C. Phaff, C. H. W. Swüste, W. J. M. de Jonge, R. Hoogerbeets, and A. J. van Duyneveldt, J. Phys. C **17**, 2583 (1984).
[17]E. Magyari and H. Thomas, J. Phys. C **15**, L333 (1982).
[18]T. Schneider and E. Stoll, Phys. Rev. B **22**, 5317 (1980).
[19]K. Sasaki and T. Tsuzuki, Solid State Commun. **41**, 521 (1982).
[20]F. Borsa, M. G. Pini, A. Rettori, and V. Tognetti, Phys. Rev. B **28**, 5173 (1983).
[21]K. Sasaki and T. Tsuzuki, J. Magn. Magn. Mater. **31-34**, 1283 (1983).
[22]K. M. Leung and A. R. Bishop, J. Phys. C **16**, 5893 (1983).

[23]H. C. Fogedby, P. Hedegård, and A. Svane, Phys. Rev. B **28**, 2893 (1983).
[24]H. J. Mikeska and K. Osano, Z. Phys. B **52**, 111 (1983).
[25]F. Boersma, K. Kopinga, and W. J. M. de Jonge, Phys. Rev. B **23**, 186 (1981).
[26]M. E. Fisher, Am. J. Phys. **32**, 343 (1964).
[27]K. Maki, Phys. Rev. B **24**, 3991 (1981).
[28]H. J. Mikeska, Phys. Rev. B **26**, 5213 (1982).
[29]P. S. Riseborough, Solid State Commun. **48**, 901 (1983).
[30]G. Wysin, A. R. Bishop, and P. Kumar, J. Phys. C **17**, 5975 (1984).
[31]E. Lieb, T. Schultz, and D. Mattis, Ann. Phys. (N.Y.) **16**, 407 (1961).
[32]H. J. Mikeska, J. Appl. Phys. **52**, 1950 (1981).
[33]S. Katsura, Phys. Rev. **127**, 1508 (1962).
[34]A. C. Phaff, C. H. W. Swüste, K. Kopinga, and W. J. M. de Jonge, J. Phys. C **16**, 6635 (1983).
[35]M. Fowler, N. F. Wright, and M. D. Johnson, *Is TMMC a sine-Gordon System?,* Vol. 54 of *Springer Series in Solid State Sciences* (Springer, Berlin, 1984), p. 99.
[36]I. U. Heilmann, J. K. Kjems, Y. Endoh, G. F. Reiter, G. Shirane, and R. J. Birgeneau, Phys. Rev. B **24**, 3939 (1981).